A BERNSTEIN-BÉZIER BASIS FOR ARBITRARY ORDER RAVIART-THOMAS FINITE ELEMENTS

MARK AINSWORTH, GAELLE ANDRIAMARO, AND OLEG DAVYDOV

Abstract. A Bernstein-Bézier basis is developed for $\boldsymbol{H}(\mathrm{div})$-conforming finite elements that gives a clear separation between the *curls* of the Bernstein basis for the polynomial discretisation of the space H^1, and the non-curls that characterize the specific $\boldsymbol{H}(\mathrm{div})$ finite element space (Raviart-Thomas in our case). The resulting basis has two distinct components reflecting this separation with the basis functions in each component having a natural identification with a domain point, or node, on the element. It is shown that the basis retains the favourable properties of the Bernstein basis that were used in [1] to develop efficient computational procedures for the application of the elements.

1. Introduction

Given the advanced state of the theory and application of spline approximation techniques, the impact on finite element analysis is surprisingly minor given the central role that piecewise polynomial approximation plays in finite element approximation. Although links between spline approximation and finite element analysis have been long known [18, 19], the advent of so-called *iso-geometric* finite element analysis [6, 13] has led to a burgeoning of interest in developing links between spline approximation, CAGD techniques and finite element analysis.

Bernstein polynomials play an important role in CAGD [15] and possess a number of interesting properties that have led to their widespread usage in a range of applications [10]. Historically, hierarchic polynomial bases [21] have been used virtually exclusively for high order finite element approximation. However, the Bernstein basis is more natural with the degrees of freedom being more akin to the nodal degrees of freedom described in most finite element textbooks. More importantly, it was recently shown that using a Bernstein basis for the standard H^1-conforming finite element spaces enables the mass and stiffness matrices to be constructed in optimal complexity [1] in terms of the polynomial degree. The algorithms take advantage of properties of Bernstein polynomials and the *sum-factorisation* approach that provides the cornerstone of the spectral method [16].

The purpose of the present work is to extend the ideas of [1, 14] to the case of conforming finite element approximation of the space $\boldsymbol{H}(\mathrm{div})$ on triangulations. Bernstein polynomials have been used to construct bases for these, and more general, spaces in [4]. In the present work, following the idea in [17], we seek a basis that gives a clear separation between what are sometimes termed the *curls* of the Bernstein polynomial basis for the H^1 space, and the non-curls that characterize

1991 *Mathematics Subject Classification.* 65N30.

Key words and phrases. spectral/*hp* finite element; Bernstein polynomials.

Support for MA under AFOSR contract FA9550-12-1-0399 is gratefully acknowledged. The work of GA was supported in part by SORSAS.

the specific $\boldsymbol{H}(\mathrm{div})$ finite element space (Raviart-Thomas in our case). The resulting basis has two distinct components reflecting this separation with the basis functions in each component having a natural identification with a domain point, or node, on the reference element in contrast with the hierarchic finite element bases developed hitherto [2, 8]. More importantly, it is shown that the basis retains the favourable properties of the Bernstein basis that were used in [1] to develop efficient computational procedures for the application of the elements.

The remainder of the text is organised as follows. We begin by summarising some key properties of Bernstein polynomials that will be needed in the analysis. The main part of the paper then deals with the construction of the basis, a study of its properties and its geometric interpretation. Attention is then turned to using the basis in practical computations.

2. Notations and Preliminaries

Standard multi-index notations will be used throughout. In particular, for $\boldsymbol{\alpha} \in \mathbb{Z}^d_+$, we define $|\boldsymbol{\alpha}| = \sum_{k=1}^d \alpha_k$, $\boldsymbol{\alpha}! = \prod_{k=1}^d \alpha_k!$ and $\binom{|\boldsymbol{\alpha}|}{\boldsymbol{\alpha}} = |\boldsymbol{\alpha}|!/\boldsymbol{\alpha}!$. If $\boldsymbol{x} \in \mathbb{R}^d$, then we define $\boldsymbol{x}^{\boldsymbol{\alpha}} = \prod_{k=1}^d x_k^{\alpha_k}$. Given a pair $\boldsymbol{\alpha}, \boldsymbol{\beta} \in \mathbb{Z}^d_+$, $\boldsymbol{\beta} \le \boldsymbol{\alpha}$ if and only if $\beta_k \le \alpha_k$, $k = 1, \ldots, d$ and, in this case, $\binom{\boldsymbol{\alpha}}{\boldsymbol{\beta}} = \prod_{k=1}^d \binom{\alpha_k}{\beta_k}$. An indexing set $\mathcal{I}_n$ is defined by

$$\mathcal{I}_n = \left\{ \boldsymbol{\alpha} \in \mathbb{Z}^3_+ : \ |\boldsymbol{\alpha}| = n \right\}. \tag{1}$$

Let $\boldsymbol{e}_\ell \in \mathcal{I}_1$ denote the multi-index whose ℓ-th entry is unity and whose remaining entries vanish.

Let T be a non-degenerate triangle with vertices $\boldsymbol{x}_1$, $\boldsymbol{x}_2$, $\boldsymbol{x}_3$ ordered in an anti-clockwise sense. The set $\mathcal{D}_n(T) = \{\boldsymbol{x}_{\boldsymbol{\alpha}} : \boldsymbol{\alpha} \in \mathcal{I}_n\}$ consists of the *domain points* of T defined by

$$\boldsymbol{x}_{\boldsymbol{\alpha}} = \frac{1}{n} \sum_{k=1}^3 \alpha_k \boldsymbol{x}_k \tag{2}$$

The *barycentric coordinates* of a point $\boldsymbol{x} \in \mathbb{R}^2$ with respect to the triangle T are given by $\boldsymbol{\lambda} = (\lambda_1, \lambda_2, \lambda_3)$ where

$$\boldsymbol{x} = \sum_{k=1}^3 \lambda_k \boldsymbol{x}_k; \quad 1 = \sum_{k=1}^3 \lambda_k. \tag{3}$$

The Bernstein polynomials of degree $n \in \mathbb{Z}_+$ associated with T are defined by

$$B^n_{\boldsymbol{\alpha}}(\boldsymbol{x}) = \binom{n}{\boldsymbol{\alpha}} \boldsymbol{\lambda}^{\boldsymbol{\alpha}}, \quad \boldsymbol{\alpha} \in \mathcal{I}_n, \tag{4}$$

and can be shown to form a partition of unity:

$$\sum_{\boldsymbol{\alpha} \in \mathcal{I}_n} B^n_{\boldsymbol{\alpha}} = 1. \tag{5}$$

The following property is an easy consequence of definition (4):

$$\lambda_k B^n_{\boldsymbol{\alpha}} = \frac{\alpha_k + 1}{n+1} B^{n+1}_{\boldsymbol{\alpha}+\boldsymbol{e}_k}, \quad k \in \{1, 2, 3\}, \quad \boldsymbol{\alpha} \in \mathcal{I}_n. \tag{6}$$

On summing the above identity over k and recalling (3), we obtain

$$B^n_{\boldsymbol{\alpha}} = \sum_{k=1}^3 \frac{\alpha_k + 1}{n+1} B^{n+1}_{\boldsymbol{\alpha}+\boldsymbol{e}_k}, \quad \boldsymbol{\alpha} \in \mathcal{I}_n. \tag{7}$$

Alternatively, summing (6) over $\boldsymbol{\alpha}$ and recalling (5) gives

$$\sum_{\boldsymbol{\alpha}\in\mathcal{I}_{n+1}} \alpha_k B^{n+1}_{\boldsymbol{\alpha}} = (n+1)\lambda_k, \quad k \in \{1,2,3\}. \tag{8}$$

Given a smooth vector-valued function $\boldsymbol{f} = (f_1, f_2)$, let $\boldsymbol{f}^\perp = (-f_2, f_1)$ and $\operatorname{curl} \boldsymbol{f} = \partial f_2/\partial x_1 - \partial f_1/\partial x_2$, whilst for a smooth scalar-valued function ϕ, denote $\mathbf{curl}\,\phi = (\partial\phi/\partial x_2, -\partial\phi/\partial x_1)$. In particular, observe that

$$\mathbf{grad}\,\lambda_k = -\frac{|\gamma_k|}{2|T|}\boldsymbol{n}_k \tag{9}$$

where $\boldsymbol{n}_k$ is the unit outward normal on the edge γ_k of the triangle T opposite to the vertex $\boldsymbol{x}_k$, and $|T|$ and $|\gamma_k|$ denote the area and length of the element and the face respectively. Equally well,

$$\mathbf{curl}\,\lambda_k = \frac{|\gamma_k|}{2|T|}\boldsymbol{t}_k \tag{10}$$

where $\boldsymbol{t}_k$ is the unit (positively oriented) tangent vector on the side γ_k.

The following identity will be useful later:

$$\mathbf{curl}\, B^{n+1}_{\boldsymbol{\alpha}} = (n+1)\sum_{k=1}^{3} B^{n}_{\boldsymbol{\alpha}-\boldsymbol{e}_k}\,\mathbf{curl}\,\lambda_k, \quad \boldsymbol{\alpha}\in\mathcal{I}_{n+1} \tag{11}$$

along with the corresponding identity with **curl** replaced by **grad**. It is worth pointing out that in (11) and hereafter, we shall frequently make use of the convention whereby terms corresponding to multi-indices with negative components are ignored (taken to be zero). Substituting for the Bernstein polynomial in the right hand side and using identity (7) gives the alternative expression

$$\mathbf{curl}\, B^{n+1}_{\boldsymbol{\alpha}} = \sum_{k,\ell=1}^{3} (1+\alpha_\ell - \delta_{k\ell}) B^{n+1}_{\boldsymbol{\alpha}+\boldsymbol{e}_\ell-\boldsymbol{e}_k}\,\mathbf{curl}\,\lambda_k, \quad \boldsymbol{\alpha}\in\mathcal{I}_{n+1}. \tag{12}$$

3. Bernstein-Bézier $\boldsymbol{H}(\mathrm{div})$ Finite Element

The function space

$$\boldsymbol{H}(\mathrm{div};\Omega) = \{\boldsymbol{v}\in L^2(\Omega)\times L^2(\Omega) : \operatorname{div}\boldsymbol{v}\in L^2(\Omega)\} \tag{13}$$

arises naturally in the modelling of many problems were there is an underlying conservation principle. For instance, Darcy's law for the flow of a viscous fluid in a permeable medium relates the velocity field $\boldsymbol{u}$ to the pressure p and the gravity vector $\boldsymbol{g}$ according to

$$\boldsymbol{u} = -\frac{\kappa}{\nu}\left(\mathbf{grad}\,p + \varrho\boldsymbol{g}\right) \text{ in } \Omega$$

where $\nu > 0$ is the viscosity, ϱ is the density and $\kappa > 0$ is the permeability. Conservation of mass means that

$$\operatorname{div}\boldsymbol{u} = f \text{ in } \Omega$$

where f is the volumetric flow rate. The normal flux $\boldsymbol{n}\cdot\boldsymbol{u} = \psi$ is specified on the domain boundary $\partial\Omega$ and the pressure normalised to have average value equal to

zero. The variational form of this problem consists of finding $(\boldsymbol{u}, p) \in \boldsymbol{H}(\mathrm{div};\Omega) \times L^2_0(\Omega)$ such that $\boldsymbol{n}\cdot\boldsymbol{u} = \psi$ on $\partial\Omega$ and

$$\begin{aligned} \frac{\nu}{\kappa}(\boldsymbol{u},\boldsymbol{v}) - (p, \mathrm{div}\,\boldsymbol{v}) &= -\varrho(\boldsymbol{g},\boldsymbol{v}) \\ (\mathrm{div}\,\boldsymbol{u}, w) &= (f, w) \end{aligned} \tag{14}$$

for all $(\boldsymbol{v}, w) \in \boldsymbol{H}_0(\mathrm{div};\Omega) \times L^2_0(\Omega)$, where $\boldsymbol{H}_0(\mathrm{div};\Omega) = \{\boldsymbol{v} \in \boldsymbol{H}(\mathrm{div};\Omega) : \boldsymbol{n}\cdot\boldsymbol{v} = 0 \text{ on } \partial\Omega\}$ and $L^2_0(\Omega) = \{w \in L^2(\Omega) : \int_\Omega w\,\mathrm{d}\boldsymbol{x} = 0\}$.

In two dimensions, the space $\boldsymbol{H}(\mathrm{div})$ is isomorphic to the space $\boldsymbol{H}(\mathrm{curl})$ defined by replacing the div-operator by the curl-operator in definition (13), under the isomorphism $\boldsymbol{\sigma} \to \boldsymbol{\sigma}^\perp$. This fact can be exploited to formulate electromagnetic problems in $\boldsymbol{H}(\mathrm{div})$. Consider the time-harmonic Maxwell

$$\nabla\times\boldsymbol{E} = -i\omega\boldsymbol{B}; \quad \nabla\times\boldsymbol{B} = i\frac{\omega}{c^2}\boldsymbol{E}; \quad \mathrm{div}\,\boldsymbol{E} = 0; \quad \mathrm{div}\,\boldsymbol{B} = 0$$

and $\boldsymbol{t}\cdot\boldsymbol{E} = \boldsymbol{0}$ on $\partial\Omega$, where c is the speed of light in vacuo, ω is the temporal frequency and $\boldsymbol{t}$ is the unit tangent on $\partial\Omega$. Eliminating the magnetic field $\boldsymbol{B}$ in favour of the electric field $\boldsymbol{E}$ gives rise to

$$\mathbf{curl}(\mathrm{curl}\,\boldsymbol{E}) = k^2\boldsymbol{E}; \quad \mathrm{div}\,\boldsymbol{E} = 0$$

where $k = \omega/c$ is the wave-number. Letting $\boldsymbol{u} = \boldsymbol{E}^\perp$ transforms the problem to the equivalent form

$$-\mathbf{grad}(\mathrm{div}\,\boldsymbol{u}) = k^2\boldsymbol{u}; \quad \mathrm{curl}\,\boldsymbol{u} = 0$$

with $\boldsymbol{n}\cdot\boldsymbol{u} = 0$ on $\partial\Omega$. The variational form of the above problem consists of seekfing $\boldsymbol{u} \in \boldsymbol{H}_0(\mathrm{div};\Omega)$ such that

$$(\mathrm{div}\,\boldsymbol{u}, \mathrm{div}\,\boldsymbol{v}) - k^2(\boldsymbol{u},\boldsymbol{v}) = 0$$

for all $\boldsymbol{v} \in \boldsymbol{H}_0(\mathrm{div};\Omega)$. This is a classic eigenvalue problem where the use of nodal finite elements results in spurious eigenvalues [12] which are not present if a conforming finite element discretisation of $\boldsymbol{H}(\mathrm{div})$ is used.

3.1. **Raviart-Thomas Finite Element Space.** A conforming finite element discretisation of the space $\boldsymbol{H}(\mathrm{div};\Omega)$ entails the use of vector-valued piecewise polynomial functions that have continuous normal components across element interfaces. Although many choices of suitable spaces are available [5], we focus our attention on the Raviart-Thomas spaces of any polynomial order.

Let $\mathbb{P}_n$ denote the space of bivariate polynomials of total degree at most n and let $\mathbb{P}^2_n$ denote the space of vector functions whose components are polynomials in $\mathbb{P}_n$. The *Raviart-Thomas* finite element $\mathbb{RT}_n$ of order $n \in \mathbb{Z}_+$ is defined by

$$\mathbb{RT}_n = \mathbb{P}^2_n + \boldsymbol{x}\mathbb{P}_n$$

and has dimension $(n+1)(n+3)$.

In particular, the lowest order space $\mathbb{RT}_0$ has dimension 3 and contains the functions

$$\boldsymbol{\omega}_k = \frac{1}{2|T|}(\boldsymbol{x} - \boldsymbol{x}_k), \quad k = 1, 2, 3. \tag{15}$$

These functions have constant normal components on the element edges satisfying

$$\boldsymbol{n}_k\cdot\boldsymbol{\omega}_\ell|_{\gamma_k} = \begin{cases} 1/|\gamma_k| & \text{if } k = \ell \\ 0 & \text{otherwise} \end{cases} \tag{16}$$

for $k, \ell \in \{1, 2, 3\}$. An immediate consequence is that the functions are linearly independent, and so the space $V_{\boldsymbol{\omega}} = \text{span}\{\boldsymbol{\omega}_k : k = 1, 2, 3\}$ coincides with $\mathbb{RT}_0$. Identities (3) and (10) readily show that these functions may be written in the form of (rotated) *Whitney functions*

$$\begin{aligned} \boldsymbol{\omega}_1 &= \lambda_2 \,\mathbf{curl}\, \lambda_3 - \lambda_3 \,\mathbf{curl}\, \lambda_2 \\ \boldsymbol{\omega}_2 &= \lambda_3 \,\mathbf{curl}\, \lambda_1 - \lambda_1 \,\mathbf{curl}\, \lambda_3 \\ \boldsymbol{\omega}_3 &= \lambda_1 \,\mathbf{curl}\, \lambda_2 - \lambda_2 \,\mathbf{curl}\, \lambda_1. \end{aligned} \tag{17}$$

Observe that these functions may be expressed in the form of a determinant:

$$\boldsymbol{\omega}_1 = \begin{vmatrix} 1 & 0 & 0 \\ \lambda_1 & \lambda_2 & \lambda_3 \\ \mathbf{curl}\, \lambda_1 & \mathbf{curl}\, \lambda_2 & \mathbf{curl}\, \lambda_3 \end{vmatrix} \tag{18}$$

with similar expressions for $\boldsymbol{\omega}_2$ and $\boldsymbol{\omega}_3$.

In search of a convenient basis for higher order Raviart-Thomas spaces $\mathbb{RT}_n$, $n \in \mathbb{Z}_+$, we define a function $\boldsymbol{\Upsilon}^n_{\boldsymbol{\alpha}}$ by the rule

$$\boldsymbol{\Upsilon}^n_{\boldsymbol{\alpha}} = (n+1) B^n_{\boldsymbol{\alpha}} \begin{vmatrix} \alpha_1 & \alpha_2 & \alpha_3 \\ \lambda_1 & \lambda_2 & \lambda_3 \\ \mathbf{curl}\, \lambda_1 & \mathbf{curl}\, \lambda_2 & \mathbf{curl}\, \lambda_3 \end{vmatrix}, \quad \boldsymbol{\alpha} \in \mathcal{I}_n. \tag{19}$$

Some useful properties of these functions are collected in the following result.

Lemma 3.1. *The functions* $\{\boldsymbol{\Upsilon}^n_{\boldsymbol{\alpha}} : \boldsymbol{\alpha} \in \mathcal{I}_n\}$ *belong to* $\mathbb{RT}_n$ *and have vanishing normal component on the boundary of the triangle* T*. Moreover, the following statements are equivalent:*

(i) $\sum_{\boldsymbol{\alpha} \in \mathcal{I}_n} c_{\boldsymbol{\alpha}} \boldsymbol{\Upsilon}^n_{\boldsymbol{\alpha}} = \mathbf{0}$,

(ii) $\text{div}\left(\sum_{\boldsymbol{\alpha} \in \mathcal{I}_n} c_{\boldsymbol{\alpha}} \boldsymbol{\Upsilon}^n_{\boldsymbol{\alpha}}\right) = 0$,

(iii) $\exists c \in \mathbb{R} : c_{\boldsymbol{\alpha}} = c, \quad \forall \boldsymbol{\alpha} \in \mathcal{I}_n$.

Proof. Expanding the determinant in (19) by the first row gives

$$\boldsymbol{\Upsilon}^n_{\boldsymbol{\alpha}} = (n+1) B^n_{\boldsymbol{\alpha}} \left(\alpha_1 \boldsymbol{\omega}_1 + \alpha_2 \boldsymbol{\omega}_2 + \alpha_3 \boldsymbol{\omega}_3\right) \tag{20}$$

and, on recalling $\boldsymbol{\omega}_k \in \mathbb{RT}_0$, it follows at once that $\boldsymbol{\Upsilon}^n_{\boldsymbol{\alpha}} \in \mathbb{RT}_n$. Since the barycentric coordinate λ_k vanishes on edge γ_k, the function $\alpha_k \lambda_k^{\alpha_k}$ also vanishes on γ_k for all values of $\alpha_k \in \mathbb{Z}_+$. As a result, $\alpha_k B^n_{\boldsymbol{\alpha}}$ vanishes on γ_k and, recalling property (16) of the Whitney functions and using the previous identity, we conclude that the normal component of $\boldsymbol{\Upsilon}^n_{\boldsymbol{\alpha}}$ vanishes on the entire element boundary.

Clearly (i) $\Rightarrow$ (ii). The proof that (ii) $\Rightarrow$ (iii) requires some preparation. Making use of identity (6) and the representation (19) allows $\boldsymbol{\Upsilon}^n_{\boldsymbol{\alpha}}$ to be expressed purely in terms of Bernstein polynomials as follows:

$$\boldsymbol{\Upsilon}^n_{\boldsymbol{\alpha}} = \begin{vmatrix} \alpha_1 & \alpha_2 & \alpha_3 \\ (1+\alpha_1) B^{n+1}_{\boldsymbol{\alpha}+\boldsymbol{e}_1} & (1+\alpha_2) B^{n+1}_{\boldsymbol{\alpha}+\boldsymbol{e}_2} & (1+\alpha_3) B^{n+1}_{\boldsymbol{\alpha}+\boldsymbol{e}_3} \\ \mathbf{curl}\, \lambda_1 & \mathbf{curl}\, \lambda_2 & \mathbf{curl}\, \lambda_3 \end{vmatrix}. \tag{21}$$

Expanding the determinant by the second row shows that $\boldsymbol{\Upsilon}^n_{\boldsymbol{\alpha}}$ may be written as a sum of three terms of the form

$$(1+\alpha_1) B^{n+1}_{\boldsymbol{\alpha}+\boldsymbol{e}_1} \left(\alpha_3 \,\mathbf{curl}\, \lambda_2 - \alpha_2 \,\mathbf{curl}\, \lambda_3\right). \tag{22}$$

A straightforward computation using (11) with **curl** replaced by **grad** reveals that

$$\mathbf{grad}\, B^{n+1}_{\boldsymbol{\alpha}+\boldsymbol{e}_1} = (n+1)\left\{B^n_{\boldsymbol{\alpha}}\,\mathbf{grad}\,\lambda_1 + B^n_{\boldsymbol{\alpha}+\boldsymbol{e}_1-\boldsymbol{e}_2}\,\mathbf{grad}\,\lambda_2 + B^n_{\boldsymbol{\alpha}+\boldsymbol{e}_1-\boldsymbol{e}_3}\,\mathbf{grad}\,\lambda_3\right\}$$

which, along with $\mathbf{grad}\,\lambda_1\cdot\mathbf{curl}\,\lambda_2 = \mathbf{grad}\,\lambda_2\cdot\mathbf{curl}\,\lambda_3 = \mathbf{grad}\,\lambda_3\cdot\mathbf{curl}\,\lambda_1 = 1/2|T|$ and $\mathbf{grad}\,\lambda_2\cdot\mathbf{curl}\,\lambda_1 = \mathbf{grad}\,\lambda_3\cdot\mathbf{curl}\,\lambda_2 = \mathbf{grad}\,\lambda_1\cdot\mathbf{curl}\,\lambda_3 = -1/2|T|$, shows that the divergence of the expression (22) is given by

$$\frac{n+1}{2|T|}(1+\alpha_1)\left\{(\alpha_2+\alpha_3)B^n_{\boldsymbol{\alpha}} - \alpha_2 B^n_{\boldsymbol{\alpha}+\boldsymbol{e}_1-\boldsymbol{e}_2} - \alpha_3 B^n_{\boldsymbol{\alpha}+\boldsymbol{e}_1-\boldsymbol{e}_3}\right\}.$$

Summing this expression and the corresponding expressions for the remaining two terms, gives the following identity

$$\begin{aligned}\operatorname{div}\boldsymbol{\Upsilon}^n_{\boldsymbol{\alpha}} = \frac{n+1}{2|T|}\Big\{\quad & 2(n+\alpha_1\alpha_2+\alpha_2\alpha_3+\alpha_3\alpha_1)B^n_{\boldsymbol{\alpha}} \\ & -(1+\alpha_1)\alpha_2 B^n_{\boldsymbol{\alpha}+\boldsymbol{e}_1-\boldsymbol{e}_2} - (1+\alpha_1)\alpha_3 B^n_{\boldsymbol{\alpha}+\boldsymbol{e}_1-\boldsymbol{e}_3} \\ & -(1+\alpha_2)\alpha_3 B^n_{\boldsymbol{\alpha}+\boldsymbol{e}_2-\boldsymbol{e}_3} - (1+\alpha_2)\alpha_1 B^n_{\boldsymbol{\alpha}+\boldsymbol{e}_2-\boldsymbol{e}_1} \\ & -(1+\alpha_3)\alpha_1 B^n_{\boldsymbol{\alpha}+\boldsymbol{e}_3-\boldsymbol{e}_1} - (1+\alpha_3)\alpha_2 B^n_{\boldsymbol{\alpha}+\boldsymbol{e}_3-\boldsymbol{e}_2}\Big\}.\end{aligned} \tag{23}$$

With the aid of this identity, we obtain

$$\operatorname{div}\left(\sum_{\boldsymbol{\alpha}\in\mathcal{I}_n} c_{\boldsymbol{\alpha}}\boldsymbol{\Upsilon}^n_{\boldsymbol{\alpha}}\right) = \sum_{\boldsymbol{\alpha}\in\mathcal{I}_n}\widetilde{c}_{\boldsymbol{\alpha}}B^n_{\boldsymbol{\alpha}} \tag{24}$$

where

$$\begin{aligned}\widetilde{c}_{\boldsymbol{\alpha}} = \frac{n+1}{2|T|}\Big\{\quad & 2(n+\alpha_1\alpha_2+\alpha_2\alpha_3+\alpha_3\alpha_1)c_{\boldsymbol{\alpha}} \\ & -\alpha_1(1+\alpha_2)c_{\boldsymbol{\alpha}-\boldsymbol{e}_1+\boldsymbol{e}_2} - \alpha_1(1+\alpha_3)c_{\boldsymbol{\alpha}-\boldsymbol{e}_1+\boldsymbol{e}_3} \\ & -\alpha_2(1+\alpha_3)c_{\boldsymbol{\alpha}-\boldsymbol{e}_2+\boldsymbol{e}_3} - \alpha_2(1+\alpha_1)c_{\boldsymbol{\alpha}-\boldsymbol{e}_2+\boldsymbol{e}_1} \\ & -\alpha_3(1+\alpha_1)c_{\boldsymbol{\alpha}-\boldsymbol{e}_3+\boldsymbol{e}_1} - \alpha_3(1+\alpha_2)c_{\boldsymbol{\alpha}-\boldsymbol{e}_3+\boldsymbol{e}_2}\Big\}.\end{aligned} \tag{25}$$

Suppose that condition (ii) holds, then $\sum_{\boldsymbol{\alpha}\in\mathcal{I}_n}\widetilde{c}_{\boldsymbol{\alpha}}B^n_{\boldsymbol{\alpha}} = 0$. The linear independence of the Bernstein polynomials means that $\widetilde{c}_{\boldsymbol{\alpha}} = 0$ for all $\boldsymbol{\alpha}\in\mathcal{I}_n$. This latter condition constitutes a square linear system for the coefficients $c_{\boldsymbol{\alpha}}$. The system is irreducible and weakly diagonally dominant, with the coefficients in each row of the system summing to zero. Hence, there exists $c\in\mathbb{R}$ such that $c_{\boldsymbol{\alpha}} = c$ for all $\boldsymbol{\alpha}\in\mathcal{I}_n$. Consequently, (ii) $\Rightarrow$ (iii).

Observe that the implication (iii) $\Rightarrow$ (i) is equivalent to $\sum_{\boldsymbol{\alpha}\in\mathcal{I}_n}\boldsymbol{\Upsilon}^n_{\boldsymbol{\alpha}} = \mathbf{0}$. Making use of the representation (20) along with identity (8) with $n+1$ replaced by n, gives

$$\sum_{\boldsymbol{\alpha}\in\mathcal{I}_n}\boldsymbol{\Upsilon}^n_{\boldsymbol{\alpha}} = n(n+1)\left(\lambda_1\boldsymbol{\omega}_1+\lambda_2\boldsymbol{\omega}_2+\lambda_3\boldsymbol{\omega}_3\right).$$

Simple algebra then suffices to show that the final term in parentheses vanishes. □

The following consequence of Lemma 3.1 will be useful:

Theorem 3.2. *Let $\mathcal{I}'_n$ denote the set obtained when a single, arbitrary index is omitted from the set $\mathcal{I}_n$. Then, the space $V^n_{\boldsymbol{\Upsilon}} = \operatorname{span}\{\boldsymbol{\Upsilon}^n_{\boldsymbol{\alpha}} : \boldsymbol{\alpha}\in\mathcal{I}'_n\}$ consists of $n(n+3)/2$ linearly independent functions belonging to $\mathbb{RT}_n\cap\boldsymbol{H}_0(\operatorname{div};T)$. Moreover, $V^n_{\boldsymbol{\Upsilon}}\cap\mathbb{RT}_0 = \{\mathbf{0}\}$.*

Proof. The result follows at once from Lemma 3.1 and the fact that $\#\mathcal{I}'_n = \#\mathcal{I}_n - 1 = n(n+3)/2$. The final statement is an immediate consequence of the stronger result $\boldsymbol{H}_0(\mathrm{div}; T) \cap \mathbb{RT}_0 = \{\mathbf{0}\}$. □

A basis for $\mathbb{RT}_n$ can be constructed by supplementing the space $V^n_{\boldsymbol{\Upsilon}}$ with a further $\dim \mathbb{RT}_n - n(n+3)/2 = (n+2)(n+3)/2$ linearly independent functions. The required number of additional functions coincides with the dimension of the space $\mathbb{P}_{n+1}$. Can use be made of the space $\mathbb{P}_{n+1}$ to construct a basis for $\mathbb{RT}_n$? The following result is of interest in this respect:

Lemma 3.3. $V^n_{\boldsymbol{\Upsilon}} \cap \mathbf{curl}\, H^1(T) = \{\mathbf{0}\}$.

Proof. Suppose the result is false and there exists $\chi \in H^1$ such that $\mathbf{curl}\,\chi \in V^n_{\boldsymbol{\Upsilon}}$ is non-zero. We can therefore find constants $c_{\boldsymbol{\alpha}} \in \mathbb{R}$ such that $\mathbf{curl}\,\chi = \sum_{\boldsymbol{\alpha}\in\mathcal{I}_n} c_{\boldsymbol{\alpha}} \boldsymbol{\Upsilon}^n_{\boldsymbol{\alpha}}$. Taking the divergence of this identity and using the implication (ii) ⇒ (i) in Lemma 3.1 gives $\mathbf{0} = \sum_{\boldsymbol{\alpha}\in\mathcal{I}_n} c_{\boldsymbol{\alpha}} \boldsymbol{\Upsilon}^n_{\boldsymbol{\alpha}} = \mathbf{curl}\,\chi$. The result follows from this contradiction. □

Lemma 3.3 suggests using the image of the space $\mathbb{P}_{n+1}$ under the **curl** operator, $\mathbf{curl}\,\mathbb{P}_{n+1}$, to augment $V^n_{\boldsymbol{\Upsilon}}$ with the required additional functions needed to obtain a basis for $\mathbb{RT}_n$. The next result shows this idea (narrowly) fails to achieve its objective:

Lemma 3.4. $\mathbf{curl}\,\mathbb{P}_{n+1} \subset \mathbb{RT}_n$ *and* $\mathbf{curl}\,\mathbb{P}_{n+1} \cap V^n_{\boldsymbol{\Upsilon}} = \{\mathbf{0}\}$. *Moreover,* $\dim(V^n_{\boldsymbol{\Upsilon}} \oplus \mathbf{curl}\,\mathbb{P}_{n+1}) = \dim \mathbb{RT}_n - 1$.

Proof. Clearly $\mathbf{curl}\,\mathbb{P}_{n+1} \subset \mathbb{P}^2_n \subset \mathbb{RT}_n$, whilst Lemma 3.3 shows that we have $V^n_{\boldsymbol{\Upsilon}} \cap \mathbf{curl}\,\mathbb{P}_{n+1} = \{\mathbf{0}\}$. The kernel of the **curl** operator coincides with $\mathbb{P}_0$, and hence $\dim \mathbf{curl}\,\mathbb{P}_{n+1} = \dim \mathbb{P}_{n+1} - \dim \mathbb{P}_0 = (n+1)(n+4)/2$. □

Evidently $V^n_{\boldsymbol{\Upsilon}} \oplus \mathbf{curl}\,\mathbb{P}_{n+1}$ is a subset of $\mathbb{RT}_n$ of codimension one. So what kind of function is missing? Note that if $\boldsymbol{\sigma} = \mathbf{curl}\,\chi$ for some $\chi \in H^1(T)$, then

$$\int_{\partial T} \boldsymbol{n} \cdot \boldsymbol{\sigma}\, \mathrm{d}s = \int_{\partial T} \boldsymbol{n} \cdot \mathbf{curl}\,\chi\, \mathrm{d}s = 0$$

thanks to the divergence theorem. This, along with the fact that elements of $V^n_{\boldsymbol{\Upsilon}}$ have vanishing normal components on ∂T, means that

$$\int_{\partial T} \boldsymbol{n} \cdot \boldsymbol{\sigma}\, \mathrm{d}s = 0 \quad \forall \boldsymbol{\sigma} \in V^n_{\boldsymbol{\Upsilon}} \oplus \mathbf{curl}\,\mathbb{P}_{n+1}. \tag{26}$$

Each of the Whitney functions $\boldsymbol{\omega}_k$ belongs to $\mathbb{RT}_n$ yet, in view of (16), satisfies

$$\int_{\partial T} \boldsymbol{n} \cdot \boldsymbol{\omega}_k\, \mathrm{d}s = 1$$

and therefore cannot belong to $V^n_{\boldsymbol{\Upsilon}} \oplus \mathbf{curl}\,\mathbb{P}_{n+1}$.

In summary, augmenting $V^n_{\boldsymbol{\Upsilon}}$ and $\mathbf{curl}\,\mathbb{P}_{n+1}$ with any one of the three possible Whitney functions produces a spanning set for $\mathbb{RT}_n$. In the interests of preserving symmetry, we choose to include all three Whitney functions. This of course, gives too many functions for a basis and, in order to compensate, the space $\mathbf{curl}\,\mathbb{P}_{n+1}$ must be pruned accordingly:

Lemma 3.5. *For $n \in \mathbb{N}_0$, let $\breve{\mathcal{I}}_n$ denote the indexing set*

$$\breve{\mathcal{I}}_n = \mathcal{I}_n - \{(n,0,0), (0,n,0), (0,0,n)\}.$$

Then, the space $V^n_{\mathbf{curl}} = \operatorname{span}\left\{\mathbf{curl}\, B^{n+1}_{\boldsymbol{\alpha}} : \ \boldsymbol{\alpha} \in \breve{\mathcal{I}}_{n+1}\right\}$ *consists of* $n(n+5)/2$ *linearly independent functions belonging to* $\mathbb{RT}_n$*. Moreover,* $V^n_{\mathbf{curl}} \cap \mathbb{RT}_0 = \{\mathbf{0}\}$.

Proof. The key observation is that all of the Bernstein polynomials $B^{n+1}_{\boldsymbol{\alpha}}$, $\boldsymbol{\alpha} \in \breve{\mathcal{I}}_{n+1}$, vanish at all element vertices. The dimension of the set is easily seen to be at most $\#\breve{\mathcal{I}}_{n+1} = \#\mathcal{I}_{n+1} - 3 = n(n+5)/2$, and it therefore suffices to show the functions are linearly independent. Suppose that $\mathbf{0} = \sum_{\boldsymbol{\alpha}\in\breve{\mathcal{I}}_{n+1}} c_{\boldsymbol{\alpha}}\, \mathbf{curl}\, B^{n+1}_{\boldsymbol{\alpha}} = \mathbf{curl}\left(\sum_{\boldsymbol{\alpha}\in\breve{\mathcal{I}}_{n+1}} c_{\boldsymbol{\alpha}} B^{n+1}_{\boldsymbol{\alpha}}\right)$. Then, $\sum_{\boldsymbol{\alpha}\in\breve{\mathcal{I}}_{n+1}} c_{\boldsymbol{\alpha}} B^{n+1}_{\boldsymbol{\alpha}} = c$, for some constant $c \in \mathbb{R}$. Evaluating this identity at any vertex of T gives $c = 0$ thanks to the earlier observation. The linear independence of the Bernstein polynomials then gives $c_{\boldsymbol{\alpha}} = 0$ for all $\boldsymbol{\alpha} \in \breve{\mathcal{I}}_{n+1}$.

Suppose that there exists a non-zero $\boldsymbol{\sigma} \in V^n_{\mathbf{curl}} \cap \mathbb{RT}_0$. Now, for any edge $\gamma \subset \partial T$, there holds

$$\int_\gamma \boldsymbol{n} \cdot \mathbf{curl}\, B^{n+1}_{\boldsymbol{\alpha}}\, \mathrm{d}s = 0 \text{ for all } \boldsymbol{\alpha} \in \breve{\mathcal{I}}_{n+1}.$$

This statement follows since the integral is given by the difference of the values of $B^{n+1}_{\boldsymbol{\alpha}}$ at the endpoints of γ which, as has already been noted, vanish for $\boldsymbol{\alpha} \in \breve{\mathcal{I}}_{n+1}$. In particular, since $\boldsymbol{\sigma} \in V^n_{\mathbf{curl}}$, we have

$$\int_\gamma \boldsymbol{n} \cdot \boldsymbol{\sigma}\, \mathrm{d}s = 0, \text{ for all } \gamma \subset \partial T.$$

Viewing $\boldsymbol{\sigma}$ now as an element of $\mathbb{RT}_0$, this condition implies that $\boldsymbol{\sigma} = \mathbf{0}$ giving the desired contradiction. □

The main result can now be stated:

Theorem 3.6. *The set*

$$\{\boldsymbol{\Upsilon}^n_{\boldsymbol{\alpha}} : \ \boldsymbol{\alpha} \in \mathcal{I}'_n\} \cup \left\{\mathbf{curl}\, B^{n+1}_{\boldsymbol{\alpha}} : \ \boldsymbol{\alpha} \in \breve{\mathcal{I}}_{n+1}\right\} \cup \{\boldsymbol{\omega}_1, \boldsymbol{\omega}_2, \boldsymbol{\omega}_3\}$$

forms a basis for $\mathbb{RT}_n$.

Proof. The numbers of functions contained in the respective sets are $n(n+3)/2$, $n(n+5)/2$ and 3, giving $(n+1)(n+3) = \dim \mathbb{RT}_n$ functions in total. Theorem 3.2, Lemma 3.3 and Lemma 3.5 show that the intersection of any pair of the three spaces $V^n_{\mathbf{curl}}$, $V^n_{\boldsymbol{\Upsilon}}$ and $V_{\boldsymbol{\omega}}$, consists of just the zero element. It has already been noted that $\boldsymbol{\omega}_1$, $\boldsymbol{\omega}_2$ and $\boldsymbol{\omega}_3$ are linearly independent. Thus, the functions within each set are linearly independent (see Theorem 3.2 and Lemma 3.5). □

3.2. **Geometric Interpretation.**

3.2.1. *Case* $n = 0$. We have $\mathcal{I}'_0 = \emptyset$ and $\breve{\mathcal{I}}_1 = \emptyset$. The basis therefore reduces to the standard basis for $\mathbb{RT}_0$ consisting of the three Whitney functions $\{\boldsymbol{\omega}_1, \boldsymbol{\omega}_2, \boldsymbol{\omega}_3\}$. These functions have non-zero average normal component on the three element edges as depicted in Figure 1. On a mesh, if a pair of triangles share a common edge, the coefficients assigned to the Whitney functions from each element must be chosen to ensure continuity of normal components across the edge. Basis functions which have non-zero normal components on an edge are referred to as *edge functions* or *edge degrees of freedom.*

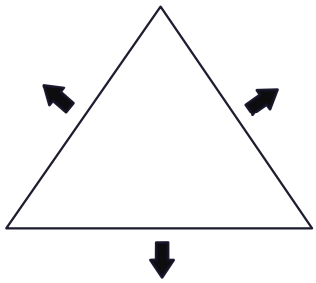

FIGURE 1. Basis functions for $\mathbb{RT}_0$ with Whitney functions indicated by arrows.

3.2.2. *Case* $n = 1$. We have $\mathcal{I}_1 = \{(1,0,0),(0,1,0),(0,0,1)\}$ with one of the indices, e.g. $(0,1,0)$, omitted from $\mathcal{I}_1$ to obtain $\mathcal{I}_1'$, and $\breve{\mathcal{I}}_2 = \{(1,1,0),(1,0,1),(0,1,1)\}$. Therefore, there are 2 basis functions from $V^1_{\boldsymbol{\Upsilon}}$, 3 functions from $V^1_{\mathbf{curl}}$ in addition to the 3 Whitney functions giving the required total of 8 basis functions for $\mathbb{RT}_1$. Figure 2 depicts these basis functions at locations corresponding to their indices.

Observe that in Figure 2 functions in $V^1_{\mathbf{curl}}$ are indicated by a $\bullet$ located on an edge. This corresponds to the function having non-zero normal components on the particular edge (but vanishing normal components on the remaining edges). For instance, the basis function associated with $\boldsymbol{\alpha} = (0,1,1)$ is given by

$$\mathbf{curl}\, B^2_{(0,1,1)} = \frac{1}{|T|}\left(\lambda_3|\gamma_2|\boldsymbol{t}_2 + \lambda_2|\gamma_3|\boldsymbol{t}_3\right)$$

whilst the domain point $\bullet$ associated with $\boldsymbol{\alpha}$ is located at the midpoint $\boldsymbol{x}_{\boldsymbol{\alpha}} = \frac{1}{2}(\boldsymbol{x}_2 + \boldsymbol{x}_3)$ of the edge joining vertices 2 and 3. It is readily verified that the basis function has non-zero normal component on this edge, and vanishing normal components on remaining edges. Such *edge degrees of freedom* must be treated in a similar fashion to the Whitney functions to ensure normal continuity across the particular edge indicated by $\bullet$.

Conversely, functions in $V^1_{\boldsymbol{\Upsilon}}$ are identified by points *internal* to the triangle. This reflects that the normal components of the functions vanish on the element boundary (as shown in Lemma 3.1). The support of the functions is a single triangle and as such, their coefficients can be assigned without reference to degrees of freedom on neighbouring triangles. Basis functions that have vanishing normal components on the whole of the element boundary are referred to as *internal basis functions* or *internal degrees of freedom* and are indicated by a point located on the interior of the element.

3.2.3. *Case* $n = 2$. We obtain $\mathcal{I}_2'$ from $\mathcal{I}_2$ by omitting an arbitrary index, e.g. $\boldsymbol{\alpha} = (0,1,1)$, and $\breve{\mathcal{I}}_3 = \{((2,1,0),(1,2,0),(2,0,1),(1,0,2),(0,2,1),(0,1,2),(1,1,1)\}$. There are 5 functions from $V^2_{\boldsymbol{\Upsilon}}$, 7 functions from $V^2_{\mathbf{curl}}$ along with the 3 Whitney functions giving the required total of 15 basis functions for $\mathbb{RT}_2$. These functions are depicted in Figure 3.

Once again, Lemma 3.1 shows that functions belonging to $V^2_{\boldsymbol{\Upsilon}}$ are all internal degrees of freedom and, as such, are indicated by points internal to the element. As before, several functions belonging to $V^2_{\mathbf{curl}}$ are indicated by points located on the edges of the element. However, in addition, there is now a function in

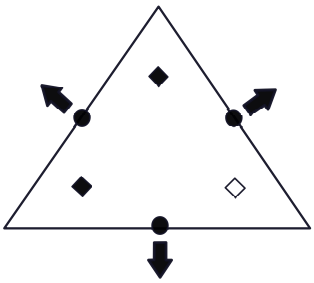

FIGURE 2. Basis functions for $\mathbb{RT}_1$: • denotes functions belonging to $V^1_{\mathbf{curl}}$; ♦ correspond to functions belonging to $V^1_{\boldsymbol{\Upsilon}}$; ◊ denotes the (arbitrarily chosen) index omitted from the set $\mathcal{I}_1$ to obtain $\mathcal{I}_1'$.

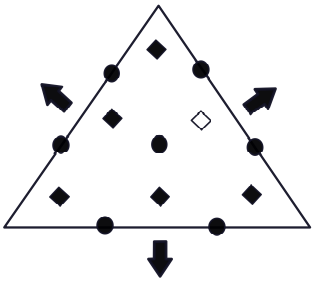

FIGURE 3. Basis functions for $\mathbb{RT}_2$: • denotes functions belonging to $V^2_{\mathbf{curl}}$; ♦ corresponds to functions belonging to $V^2_{\boldsymbol{\Upsilon}}$; ◊ denotes the (arbitrarily) chosen function omitted from the set $\mathcal{I}_2$ to obtain $\mathcal{I}_2'$.

$V^2_{\mathbf{curl}}$ associated with the index $\boldsymbol{\alpha} = (1,1,1)$ corresponding to the domain point located at the element centroid. It is not difficult to verify that the corresponding function $\mathbf{curl}\, B^3_{(1,1,1)}$ has vanishing normal components on the entire boundary and is therefore an *internal function*. Naturally, such a function is indicated by a point internal to the element. The remaining functions from $V^2_{\mathbf{curl}}$ have non-zero normal components on a single edge and are thus indicated by a point located on the edge.

3.2.4. *General Case* $n \in \mathbb{N}$. In the general case, the basis consists of the usual Whitney functions augmented with degree $n+1$ polynomial vectors written in terms of Bernstein polynomials. Lemma 3.1 shows that $V^n_{\boldsymbol{\Upsilon}}$ consists entirely of internal degrees of freedom, with basis functions identified with indices from the set $\mathcal{I}_n'$ obtained by omitting a single index from the set $\mathcal{I}_n$. The fact that the set consists entirely of internal functions means that it is irrelevant which particular index is omitted.

The set $V^n_{\mathbf{curl}}$ consists of both internal and edge degrees of freedom. The basis functions are identified with indices from the set $\breve{\mathcal{I}}_{n+1}$ obtained by omitting the vertices from the set $\mathcal{I}_{n+1}$. In this case, it is vitally important that the three omitted indices are chosen to be the element vertices in order that each resulting

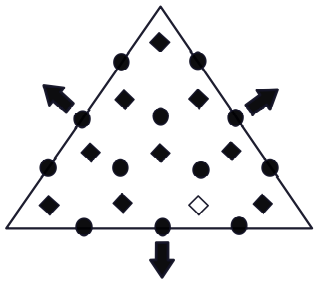

FIGURE 4. Basis functions for $\mathbb{RT}_3$: • denotes functions belonging to $V^3_{\mathbf{curl}}$; ♦ corresponds to functions belonging to $V^3_{\boldsymbol{\Upsilon}}$; ◊ denotes the (arbitrarily) chosen function omitted from the set $\mathcal{I}_3$ to obtain $\mathcal{I}'_3$.

Order	*Internal Dofs*		*Edge Dofs*		*Total*
n	$V^n_{\boldsymbol{\Upsilon}}$	$V^n_{\mathbf{curl}}$	$V_{\boldsymbol{\omega}}$	$V^n_{\mathbf{curl}}$	
0	-	-	3	-	3
1	2	-	3	3	8
2	5	1	3	6	15
3	9	3	3	9	24
⋮	⋮	⋮	⋮	⋮	⋮
n	$n(n+3)/2$	$n(n-1)/2$	3	$3n$	$(n+1)(n+3)$

TABLE 1. Number and types of degrees of freedom in the basis for $\mathbb{RT}_n$.

degree of freedom is associated with a *single edge* of the element. This would not be the case were a vertex index to be retained.

Figure 4 illustrates the case $n = 3$ where we depict the basis functions of $V^n_{\mathbf{curl}}$ by ordinary domain points x_α, $\alpha \in \breve{\mathcal{I}}_{n+1}$, and those of $V^n_{\boldsymbol{\Upsilon}}$ by

$$\bar{\boldsymbol{x}}_{\boldsymbol{\alpha}} = \frac{1}{3}\left(\boldsymbol{x}_{\boldsymbol{\alpha}+\boldsymbol{e}_1} + \boldsymbol{x}_{\boldsymbol{\alpha}+\boldsymbol{e}_2} + \boldsymbol{x}_{\boldsymbol{\alpha}+\boldsymbol{e}_3}\right), \quad \boldsymbol{\alpha} \in \mathcal{I}'_n.$$

The type and numbers of the degrees of freedom in the basis for $\mathbb{RT}_n$ are summarised in Table 1.

4. Efficient Computation with the Basis

The Darcy system (14) may be discretised using the stable finite element pairing constructed on a mesh based on using the Raviart-Thomas space $\mathbb{RT}_n$ for $\boldsymbol{H}(\mathrm{div};\Omega)$ and the standard polynomials $\mathbb{P}_n$ for $L^2(\Omega)$. The natural choice of basis for $\mathbb{P}_n$, for use in conjunction with the earlier Bernstein-Bézier basis for $\mathbb{RT}_n$, is simply to take pure Bernstein polynomials $\{B^n_{\boldsymbol{\alpha}} : \boldsymbol{\alpha} \in \mathcal{I}_n\}$.

The introduction of a basis reduces the approximation of the Darcy system to the solution of a system of linear algebraic equations which can be assembled and solved using standard finite element methodology that is applicable to any choice of basis. Earlier work [1] dealt with the use of the pure Bernstein polynomial basis in the context of the space H^1, which we now develop in the $\boldsymbol{H}(\mathrm{div})$ setting.

4.1. **Transformation to Pure Bernstein-Bézier Form.** Suppose that a finite element approximation has been computed using the basis described above, that we now wish to post-process through graphical visualisation or evaluation. Post-processing is carried out element by element and it is sufficient to consider the restriction of the approximation $\boldsymbol{u}_T$ of the velocity to a single element T written in the form

$$\boldsymbol{u}_T = \sum_{k=1}^{3} a_k \boldsymbol{\omega}_k + \sum_{\alpha \in \mathcal{I}'_n} c_{\boldsymbol{\alpha}} \boldsymbol{\Upsilon}_n + \sum_{\alpha \in \check{\mathcal{I}}_{n+1}} b_{\boldsymbol{\alpha}} \, \mathbf{curl}\, B^{n+1}_{\boldsymbol{\alpha}}.$$

In order to simplify notation, we define $c_{\boldsymbol{\alpha}} = 0$ for $\boldsymbol{\alpha} \in \mathcal{I}_n \backslash \mathcal{I}'_n$ and $b_{\boldsymbol{\alpha}} = 0$ for $\boldsymbol{\alpha} \in \mathcal{I}_{n+1} \backslash \check{\mathcal{I}}_{n+1}$, and write $\boldsymbol{u}_T$ in the form

$$\boldsymbol{u}_T = \sum_{k=1}^{3} a_k \boldsymbol{\omega}_k + \sum_{\alpha \in \mathcal{I}_n} c_{\boldsymbol{\alpha}} \boldsymbol{\Upsilon}_n + \sum_{\alpha \in \mathcal{I}_{n+1}} b_{\boldsymbol{\alpha}} \, \mathbf{curl}\, B^{n+1}_{\boldsymbol{\alpha}}. \tag{27}$$

The basis constructed in the previous section is useful for the computation of a finite element approximation from the space $\mathbb{RT}_n$, but a transformation to a standard Bernstein basis is more convenient for the purposes of post-processing, and in the fast computation of the element matrices [1]. Note that $\boldsymbol{u}_T \in \mathbb{RT}_n \subset \mathbb{P}^2_{n+1}$ so that the Bernstein polynomials of degree $n+1$ will need to be used to represent $\boldsymbol{u}_T$.

Lemma 4.1. *Let $\boldsymbol{u}_T \in \mathbb{RT}_n(T)$ be written in the form (27). Then*

$$\boldsymbol{u}_T = \sum_{\boldsymbol{\alpha} \in \mathcal{I}_{n+1}} \hat{\boldsymbol{c}}_{\boldsymbol{\alpha}} B^{n+1}_{\boldsymbol{\alpha}} \text{ and } \operatorname{div} \boldsymbol{u}_T = \frac{1}{|T|} \sum_{\boldsymbol{\alpha} \in \mathcal{I}_n} \tilde{c}_{\boldsymbol{\alpha}} B^n_{\boldsymbol{\alpha}} \tag{28}$$

where, for $\boldsymbol{\alpha} \in \mathcal{I}_{n+1}$,

$$\begin{aligned} \hat{\boldsymbol{c}}_{\boldsymbol{\alpha}} = & \sum_{k,\ell=1}^{3} \alpha_\ell b_{\boldsymbol{\alpha}+\boldsymbol{e}_k-\boldsymbol{e}_\ell} \, \mathbf{curl}\, \lambda_k \\ & + \begin{vmatrix} \alpha_1 & \alpha_2 & \alpha_3 \\ \alpha_1 c_{\boldsymbol{\alpha}-\boldsymbol{e}_1} - \dfrac{a_1}{n+1} & \alpha_2 c_{\boldsymbol{\alpha}-\boldsymbol{e}_2} - \dfrac{a_2}{n+1} & \alpha_3 c_{\boldsymbol{\alpha}-\boldsymbol{e}_3} - \dfrac{a_3}{n+1} \\ \mathbf{curl}\, \lambda_1 & \mathbf{curl}\, \lambda_2 & \mathbf{curl}\, \lambda_3 \end{vmatrix} \end{aligned} \tag{29}$$

and, for $\boldsymbol{\alpha} \in \mathcal{I}_n$,

$$\begin{aligned} \widetilde{c}_{\boldsymbol{\alpha}} = \sum_{k=1}^{3} a_k + \frac{n+1}{2} \big\{ & \quad 2(n + \alpha_1\alpha_2 + \alpha_2\alpha_3 + \alpha_3\alpha_1) c_{\boldsymbol{\alpha}} \\ & - \alpha_1(1+\alpha_2) c_{\boldsymbol{\alpha}-\boldsymbol{e}_1+\boldsymbol{e}_2} - \alpha_1(1+\alpha_3) c_{\boldsymbol{\alpha}-\boldsymbol{e}_1+\boldsymbol{e}_3} \\ & - \alpha_2(1+\alpha_3) c_{\boldsymbol{\alpha}-\boldsymbol{e}_2+\boldsymbol{e}_3} - \alpha_2(1+\alpha_1) c_{\boldsymbol{\alpha}-\boldsymbol{e}_2+\boldsymbol{e}_1} \\ & - \alpha_3(1+\alpha_1) c_{\boldsymbol{\alpha}-\boldsymbol{e}_3+\boldsymbol{e}_1} - \alpha_3(1+\alpha_2) c_{\boldsymbol{\alpha}-\boldsymbol{e}_3+\boldsymbol{e}_2} \big\}. \end{aligned} \tag{30}$$

Here, we adopt the convention whereby a coefficient with a particular index is taken to be zero if the index is out of range.

Proof. The first term in (27) can be expressed in terms of Bernstein polynomials of degree $n+1$ by making use of property (8) to obtain

$$\sum_{k=1}^{3} a_k \boldsymbol{\omega}_k = -\frac{1}{n+1} \sum_{\boldsymbol{\alpha} \in \mathcal{I}_{n+1}} B^{n+1}_{\boldsymbol{\alpha}} \begin{vmatrix} \alpha_1 & \alpha_2 & \alpha_3 \\ a_1 & a_2 & a_3 \\ \mathbf{curl}\, \lambda_1 & \mathbf{curl}\, \lambda_2 & \mathbf{curl}\, \lambda_3 \end{vmatrix}. \tag{31}$$

Identity (21) and elementary manipulation suffice to show that the second term in (27) can be written in terms of the Bernstein polynomials of degree $n+1$ as follows:

$$\sum_{\boldsymbol{\alpha}\in\mathcal{I}_{n+1}} B^{n+1}_{\boldsymbol{\alpha}} \begin{vmatrix} \alpha_1 & \alpha_2 & \alpha_3 \\ \alpha_1 c_{\boldsymbol{\alpha}-\boldsymbol{e}_1} & \alpha_2 c_{\boldsymbol{\alpha}-\boldsymbol{e}_2} & \alpha_3 c_{\boldsymbol{\alpha}-\boldsymbol{e}_3} \\ \mathbf{curl}\,\lambda_1 & \mathbf{curl}\,\lambda_2 & \mathbf{curl}\,\lambda_3 \end{vmatrix},$$

where we utilise the convention whereby $c_{\boldsymbol{\alpha}} = 0$ for $\boldsymbol{\alpha} \notin \mathcal{I}_n$. Identity (12) enables the final term in (27) to be expressed in terms of Bernstein polynomials of degree $n+1$ as follows

$$\sum_{\alpha\in\mathcal{I}_{n+1}} B^{n+1}_{\boldsymbol{\alpha}} \sum_{k,\ell=1}^{3} \alpha_\ell b_{\boldsymbol{\alpha}+\boldsymbol{e}_k-\boldsymbol{e}_\ell}\,\mathbf{curl}\,\lambda_k$$

where we again make use of the above convention. Combining the above results we may write $\boldsymbol{u}_T$ in the form (28) where the coefficients are defined by (29). The expression for the divergence of (27) is obtained as follows: definition (15) implies that the divergence of the first term is given by

$$\operatorname{div}\left(\sum_{k=1}^{3} a_k\boldsymbol{\omega}_k\right) = \frac{1}{|T|}\sum_{k=1}^{3} a_k = \frac{1}{|T|}\sum_{k=1}^{3} a_k \sum_{\boldsymbol{\alpha}\in\mathcal{I}_n} B^n_{\boldsymbol{\alpha}}$$

using property (5); the third term is divergence free; and, the divergence of the second term is obtained using (24)-(25). □

The number of operations to evaluate each of the individual coefficients $\hat{\boldsymbol{c}}_{\boldsymbol{\alpha}}$ and $\tilde{c}_{\boldsymbol{\alpha}}$ in the Bernstein representations of $\boldsymbol{u}_T$ and $\operatorname{div}\boldsymbol{u}_T$ is independent of the order n of the Raviart-Thomas space. The cost of transforming the coefficients to the Bernstein-Bézier representation is therefore directly proportional to the dimension of the local space and as such is optimal. Of course, any one of the many alternative bases for $\mathbb{RT}_n$ could be chosen and the resulting approximation again transformed to Bernstein-Bézier form; crucially the cost of the transformation would degenerate more rapidly with the order n using the above construction.

4.2. **Graphical Rendering and Post-Processing.** The evaluation of a polynomial expressed in Bernstein-Bézier form at a single point is usually obtained using the *de Casteljau* algorithm [9, 11, 15] at a cost of $\mathcal{O}(n^3)$ operations per point evaluation. The algorithm is pervasive in graphical visualisation to the extent that many graphics vendors implement the algorithm directly at hardware level accessed through *OpenGL evaluators* [7], resulting in high-performance graphical rendering. The availability of a Bernstein-Bézier representation for $\boldsymbol{u}_T$ enables these tools to be brought into play whilst incurring minimal overhead in the transformation to Bernstein-Bézier form.

Post-processing operations in finite element analysis often involve the evaluation of a functional of the approximation $\boldsymbol{u}_T$ in the form of an integral using a quadrature rule over the triangle T. A convenient quadrature rule can be defined as follows. The q-point Gauss-Jacobi quadrature rule [20]:

$$\int_0^1 (1-s)^a g(s)\,\mathrm{d}s \approx \sum_{j=1}^{q} \omega_j^{(a)} g(\xi_j^{(a)}) \tag{32}$$

has precision $2q-1$, the weights $\{\omega_j^{(a)}\}$ are all positive and the nodes $\{\xi_j^{(a)}\}$ are located on the interval $[0,1]$. The *Stroud conical product rule* [20] for a triangle T

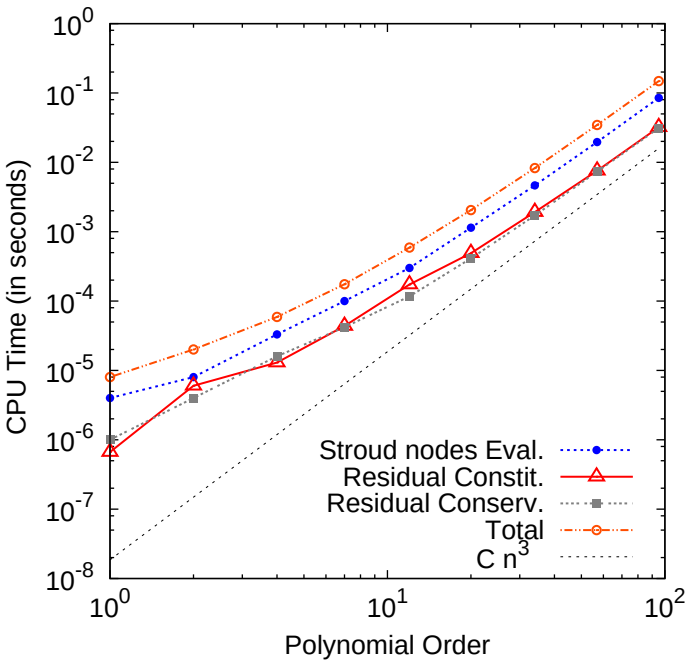

FIGURE 5. CPU times required for computation of approximation and residuals using the proposed basis.

is defined by

$$\int_T F(\boldsymbol{x}, \boldsymbol{u}, \operatorname{div} \boldsymbol{u}, \ldots)\, \mathrm{d}\boldsymbol{x} \approx 2|T| \sum_{i,j=1}^{q} \omega_i^{(1)} \omega_j^{(0)} F(\boldsymbol{x}_{i,j}, \boldsymbol{u}_{i,j}, \operatorname{div} \boldsymbol{u}_{i,j}, \ldots) \tag{33}$$

which has q^2 positive weights and nodes given by

$$\boldsymbol{x}_{i,j} = \xi_i^{(1)} \boldsymbol{x}_1 + (1 - \xi_i^{(1)}) \xi_j^{(0)} \boldsymbol{x}_2 + (1 - \xi_i^{(1)})(1 - \xi_j^{(0)}) \boldsymbol{x}_3 \tag{34}$$

for $1 \le i, j \le q$, and where $\boldsymbol{u}_{i,j} = \boldsymbol{u}(\boldsymbol{x}_{i,j})$, $\operatorname{div} \boldsymbol{u}_{i,j} = \operatorname{div} \boldsymbol{u}(\boldsymbol{x}_{i,j})$ etc.

In order to integrate a function of $\boldsymbol{u}_T$ to sufficient precision it is necessary to choose $q = \mathcal{O}(n)$. The number of quadrature points at which $\boldsymbol{u}_T$ needs to be evaluated grows as $\mathcal{O}(n^2)$. If the de Casteljau algorithm were to be employed for this purpose, then the overall cost would grow as $\mathcal{O}(n^5)$. An alternative algorithm is developed in Corollary 2 of [1] that exploits properties of the Bernstein polynomials and uses the Bernstein-Bézier coefficients to evaluate $\boldsymbol{u}_T$ at all $\mathcal{O}(n^2)$ nodes of the Stroud conical product rule at a cost of $\mathcal{O}(n^3)$ operations in total. The same complexity estimates remain valid for the evaluation of derivatives of $\boldsymbol{u}_T$, and in particular the divergence $\operatorname{div} \boldsymbol{u}_T$. Figure 5 includes timings for the evaluation of a randomly chosen vector field expressed in terms of the basis for various polynomial orders and indicating an $\mathcal{O}(n^3)$ complexity is attained.

4.3. **Assembly of Element Load Vector.** Finite element analysis of problems in $\boldsymbol{H}(\operatorname{div}; \Omega)$ involving a source term $\boldsymbol{g} : \Omega \to \mathbb{R}^2$, such as the Darcy system (14), often entails the evaluation of the element load vector whose entries are composed

of the quantities

$$\int_T \boldsymbol{g}\cdot\boldsymbol{\Upsilon}^n_{\boldsymbol{\alpha}}\,\mathrm{d}\boldsymbol{x},\quad \int_T \boldsymbol{g}\cdot\mathbf{curl}\,B^{n+1}_{\boldsymbol{\alpha}}\,\mathrm{d}\boldsymbol{x},\quad \int_T \boldsymbol{g}\cdot\boldsymbol{\omega}_k\,\mathrm{d}\boldsymbol{x} \tag{35}$$

for appropriate indices $\boldsymbol{\alpha}$ and k. These integrals generally have to be approximated using numerical quadrature. In order to avoid cluttering the notation, we shall not distinguish between the true quantities and their numerical approximation using a Stroud conical product rule of precision $q=\mathcal{O}(n)$. A central role in [1] is played by the *Bernstein-Bézier moments* of order $n+1$ of the datum $\boldsymbol{g}$ defined by

$$\mu^{n+1}_{\boldsymbol{\alpha}}(\boldsymbol{g})=\int_T \boldsymbol{g}(\boldsymbol{x})B^{n+1}_{\boldsymbol{\alpha}}(\boldsymbol{x})\,\mathrm{d}\boldsymbol{x},\quad \boldsymbol{\alpha}\in\mathcal{I}_{n+1}. \tag{36}$$

In particular, a procedure is presented in [1, Corollary 2] that enables all of these moments to be evaluated (using a Stroud conical product rule) in $\mathcal{O}(n^3)$ operations.

Once again exploiting the simple form of the Bernstein-Bézier representations of the basis functions, we are able to express the quantities (35) compactly in terms of combinations of Bernstein-Bézier moments of $\boldsymbol{g}$ as follows: using (21) gives

$$\int_T \boldsymbol{g}\cdot\boldsymbol{\Upsilon}^n_{\boldsymbol{\alpha}}\,\mathrm{d}\boldsymbol{x}=\begin{vmatrix} \alpha_1 & \alpha_2 & \alpha_3\\ (1+\alpha_1)\mu^{n+1}_{\boldsymbol{\alpha}+\boldsymbol{e}_1}(\boldsymbol{g}) & (1+\alpha_2)\mu^{n+1}_{\boldsymbol{\alpha}+\boldsymbol{e}_2}(\boldsymbol{g}) & (1+\alpha_3)\mu^{n+1}_{\boldsymbol{\alpha}+\boldsymbol{e}_3}(\boldsymbol{g})\\ \mathbf{curl}\,\lambda_1 & \mathbf{curl}\,\lambda_2 & \mathbf{curl}\,\lambda_3\end{vmatrix} \tag{37}$$

for $\boldsymbol{\alpha}\in\mathcal{I}_n$; using (12) gives

$$\int_T \boldsymbol{g}\cdot\mathbf{curl}\,B^{n+1}_{\boldsymbol{\alpha}}\,\mathrm{d}\boldsymbol{x}=\sum_{k,\ell=1}^{3}(1+\alpha_\ell-\delta_{k\ell})\mu^{n+1}_{\boldsymbol{\alpha}+\boldsymbol{e}_\ell-\boldsymbol{e}_k}(\boldsymbol{g})\cdot\mathbf{curl}\,\lambda_k \tag{38}$$

for $\boldsymbol{\alpha}\in\mathcal{I}_{n+1}$; whilst the integrals of the Whitney functions can be determined from the following identity obtained using (31),

$$\sum_{k=1}^{3}a_k\int_T \boldsymbol{g}\cdot\boldsymbol{\omega}_k\,\mathrm{d}\boldsymbol{x}=-\frac{1}{n+1}\sum_{\boldsymbol{\alpha}\in\mathcal{I}_{n+1}}\mu^{n+1}_{\boldsymbol{\alpha}}(\boldsymbol{g})\cdot\begin{vmatrix} \alpha_1 & \alpha_2 & \alpha_3\\ a_1 & a_2 & a_3\\ \mathbf{curl}\,\lambda_1 & \mathbf{curl}\,\lambda_2 & \mathbf{curl}\,\lambda_3\end{vmatrix} \tag{39}$$

valid for all a_1, a_2 and $a_3\in\mathbb{R}$.

As before, key is the fact that each term can be evaluated in $\mathcal{O}(1)$ operations meaning that the overall cost of assembling the element load vector is $\mathcal{O}(n^3)$ for the evaluation of the moments and $\mathcal{O}(n^2)$ for the transformation of the moments into entries of the load vector, giving $\mathcal{O}(n^3)$ complexity overall.

4.4. **Computation of Residuals.** The finite element approximation can be obtained through the assembly and inversion of a global algebraic system. The Bernstein-Bézier finite element basis is known [1] to yield an optimal complexity algorithm for the computation and assembly of the matrix and load vector in the H^1-setting. This result can be shown to extend to the $\boldsymbol{H}(\mathrm{div})$ case considered here [3]. However, we shall instead explore the iterative solution of the algebraic equations. Regardless of the particular choice of iterative scheme, this typically requires the elementwise evaluation of residuals in the current approximate solution $(\boldsymbol{u}^\ell,p^\ell)$:

$$\begin{aligned}\boldsymbol{v}\quad&\mapsto\quad -\varrho(\boldsymbol{g},\boldsymbol{v})_T-\frac{\nu}{\kappa}\left(\boldsymbol{u}^\ell,\boldsymbol{v}\right)_T+(p^\ell,\mathrm{div}\,\boldsymbol{v})_T\\ w\quad&\mapsto\quad (f,w)_T-(\mathrm{div}\,\boldsymbol{u}^\ell,w)_T\end{aligned}$$

where $\boldsymbol{v}$ is chosen to be $\boldsymbol{\Upsilon}^n_{\boldsymbol{\alpha}}$, $\mathbf{curl}\,B^{n+1}_{\boldsymbol{\alpha}}$ and $\boldsymbol{\omega}_k$, and $w=B^n_{\boldsymbol{\alpha}}$.

The evaluation of the element residual in the mass-conservation equation reduces to the computation of the Bernstein-Bézier moment

$$(f, B^n_{\boldsymbol{\alpha}})_T - (\operatorname{div} \boldsymbol{u}^\ell, B^n_{\boldsymbol{\alpha}})_T = \mu^n_{\boldsymbol{\alpha}}(f - \operatorname{div} \boldsymbol{u}^\ell).$$

The same methodology described in Section 4.3 for the treatment of the element load vector along with the evaluation of the (known) integrand $f - \operatorname{div} \boldsymbol{u}^\ell$ as described in Section 4.2, gives an overall complexity of $\mathcal{O}(n^3)$ for the mass-conservation residual.

The treatment of the residual in the constitutive equation

$$-\varrho(\boldsymbol{g}, \boldsymbol{v})_T - \frac{\nu}{\kappa}\left(\boldsymbol{u}^\ell, \boldsymbol{v}\right)_T + (p^\ell, \operatorname{div} \boldsymbol{v})_T = -\left(\varrho \boldsymbol{g} + \frac{\nu}{\kappa}\boldsymbol{u}^\ell, \boldsymbol{v}\right)_T + (p^\ell, \operatorname{div} \boldsymbol{v})_T$$

is slightly different. The former term is treated using Bernstein-Bézier moments as described in Section 4.3 again noting that the evaluation of the (known) function $\boldsymbol{u}^\ell$ at the quadrature points is handled as described in Section 4.2. The latter term involves contributions of the form

$$\int_T p^\ell \operatorname{div} \boldsymbol{\Upsilon}^n_{\boldsymbol{\alpha}} \,\mathrm{d}\boldsymbol{x}, \quad \int_T p^\ell \operatorname{div} \mathbf{curl}\, B^{n+1}_{\boldsymbol{\alpha}} \,\mathrm{d}\boldsymbol{x}, \quad \int_T p^\ell \operatorname{div} \boldsymbol{\omega}_k \,\mathrm{d}\boldsymbol{x} \tag{40}$$

where $p^\ell : T \mapsto \mathbb{R}$ is regarded as known data. The second of these quantities vanishes identically whilst the final quantity can be simplified by using formula (15) to replace $\operatorname{div} \boldsymbol{\omega}_k$ by $1/|T|$. The remaining quantities are amenable to the usual treatment by exploiting formula (23) to express the quantities as a linear combination of Bernstein-Bézier moments of the data p^ℓ,

$$\begin{aligned}\int_T p \operatorname{div} \boldsymbol{\Upsilon}^n_{\boldsymbol{\alpha}} \,\mathrm{d}\boldsymbol{x} = \frac{n+1}{2|T|}\Big\{ \quad & 2(n + \alpha_1\alpha_2 + \alpha_2\alpha_3 + \alpha_3\alpha_1)\mu^n_{\boldsymbol{\alpha}}(p^\ell) \\ & -(1+\alpha_1)\alpha_2\mu^n_{\boldsymbol{\alpha}+\boldsymbol{e}_1-\boldsymbol{e}_2}(p^\ell) - (1+\alpha_1)\alpha_3\mu^n_{\boldsymbol{\alpha}+\boldsymbol{e}_1-\boldsymbol{e}_3}(p^\ell) \\ & -(1+\alpha_2)\alpha_3\mu^n_{\boldsymbol{\alpha}+\boldsymbol{e}_2-\boldsymbol{e}_3}(p^\ell) - (1+\alpha_2)\alpha_1\mu^n_{\boldsymbol{\alpha}+\boldsymbol{e}_2-\boldsymbol{e}_1}(p^\ell) \\ & -(1+\alpha_3)\alpha_1\mu^n_{\boldsymbol{\alpha}+\boldsymbol{e}_3-\boldsymbol{e}_1}(p^\ell) - (1+\alpha_3)\alpha_2\mu^n_{\boldsymbol{\alpha}+\boldsymbol{e}_3-\boldsymbol{e}_2}(p^\ell)\Big\}.\end{aligned}$$

The overall complexity for the evaluation of all residuals is $\mathcal{O}(n^3)$. Figure 5 shows the timings obtained for evaluating the residuals in the conservation and constitutive equations for a range of polynomial degrees and a randomly chosen iterate p^ℓ and $\boldsymbol{u}^\ell$, and indicates that the rate $\mathcal{O}(n^3)$ is attained.

4.5. **Application to Other Problem Classes.** The developments have, so far, focused on the Darcy system but the algorithms are more generally applicable. All of the foregoing considerations regarding the use of the Bernstein-Bézier basis for the Raviart-Thomas space remain valid for the Maxwell eigenvalue problem described earlier; the details concerning the efficient treatment of the term $(\operatorname{div} \boldsymbol{u}, \operatorname{div} \boldsymbol{v})$ are left to the reader.

References

[1] M. Ainsworth, G. Andriamaro, and O. Davydov, *Bernstein-Bézier FEM and optimal assembly algorithms*, SIAM J. Sci. Comp., (2011), pp. 3087–3109.

[2] M. Ainsworth and J. Coyle, *Hierarchic finite element bases on unstructured tetrahedral meshes*, Internat. J. Numer. Methods Engrg., 58 (2003), pp. 2103–2130.

[3] G. Andriamaro, *Bernstein-Bézier Techniques in Finite Element Analysis*, PhD thesis, Strathclyde University, Glasgow, UK, 2012.

[4] D. N. Arnold, R. S. Falk, and R. Winther, *Geometric decompositions and local bases for spaces of finite element differential forms*, Comput. Methods Appl. Mech. Engrg., 198 (2009), pp. 1660–1672.
[5] F. Brezzi and M. Fortin, *Mixed and hybrid finite element methods*, Springer-Verlag, Berlin, 1991.
[6] A. Buffa, J. Rivas, G. Sangalli, and R. Vázquez, *Isogeometric discrete differential forms in three dimensions*, SIAM J. Numer. Anal., 49 (2011), pp. 818–844.
[7] T. Davis, J. Neider, and M. Woo, *OpenGL Programming Guide: The Official Guide to Learning OpenGL, Version 1.1, Second Edition*, Addison-Wesley Longman Pub (Sd), 1997.
[8] L. Demkowicz, *Computing with hp-adaptive finite elements. Vol. 1*, Chapman & Hall/CRC Applied Mathematics and Nonlinear Science Series, Chapman & Hall/CRC, Boca Raton, FL, 2007. One and two dimensional elliptic and Maxwell problems, With 1 CD-ROM (UNIX).
[9] G. Farin, *Curves and surfaces for CAGD: a practical guide, Fifth Edition*, Morgan Kaufmann Publishers Inc., San Francisco, CA, USA, 2002.
[10] R. T. Farouki, *The Bernstein polynomial basis: A centennial retrospective*, Computer Aided Geometric Design, 29 (2012), pp. 379 – 419.
[11] R. T. Farouki and V. T. Rajan, *Algorithms for polynomials in Bernstein form*, Comput. Aided Geom. Design, 5 (1988), pp. 1–26.
[12] R. Hiptmair, *Finite elements in computational electromagnetism*, Acta Numer., 11 (2002), pp. 237–339.
[13] T. J. R. Hughes and J. A. Evans, *Isogeometric analysis*, in Proceedings of the International Congress of Mathematicians. Volume I, New Delhi, 2010, Hindustan Book Agency, pp. 299–325.
[14] R. C. Kirby and K. T. Thinh, *Fast simplicial quadrature-based finite element operators using Bernstein polynomials*, Numer. Math., 121 (2012), pp. 261–279.
[15] M.-J. Lai and L. L. Schumaker, *Spline functions on triangulations*, vol. 110 of Encyclopedia of Mathematics and its Applications, Cambridge University Press, Cambridge, 2007.
[16] S. A. Orszag, *Spectral methods for problems in complex geometries*, J. Comput. Phys., 37 (1980), pp. 70–92.
[17] J. Schöberl and S. Zaglmayr, *High order Nédélec elements with local complete sequence properties*, COMPEL, 24 (2005), pp. 374–384.
[18] L. L. Schumaker, *Constructive aspects of spaces of bivariate piecewise polynomials*, in The mathematics of finite elements and applications, VI (Uxbridge, 1987), Academic Press, London, 1988, pp. 513–520.
[19] ———, *On super splines and finite elements*, SIAM J. Numer. Anal., 26 (1989), pp. 997–1005.
[20] A. H. Stroud, *Approximate calculation of multiple integrals*, Prentice-Hall Inc., Englewood Cliffs, N.J., 1971. Prentice-Hall Series in Automatic Computation.
[21] B. Szabo and I. Babuska, *Finite Element Analysis*, John Wiley & Sons, 1991.

Division of Applied Mathematics, Brown University, 182 George St, Providence RI 02912, USA.

E-mail address: Mark_Ainsworth@brown.edu

Department of Mathematics and Statistics, Strathclyde University, 26 Richmond St., Glasgow G1 1XH, Scotland.

E-mail address: {Gaelle.Andriamaro, Oleg.Davydov}@strath.ac.uk